Kinetics and Mechanism of the Heterogeneous Decomposition of Nitric Oxide on Metal Oxides in the Presence of Hydrocarbons†

A. J. Colussi* and V. T. Amorebieta

National Research Council of Argentina, P.O. Box 422, 7600-Mar del Plata, Argentina

Received: February 25, 1998; In Final Form: April 23, 1998

Rates and products of the $(3 + \alpha)NO + CH_4 \rightleftharpoons {}^1/_2(3 + \alpha)N_2 + (1 - \alpha)CO + \alpha CO_2 + 2H_2O$ $(0 \le \alpha \le 1)$ reaction were determined in low-pressure ($NO/CH_4/O_2$) mixtures ($[NO] < 1\ \mu M$, $[CH_4] < 10[NO]$, $[O_2] \le [NO]$; $1\ \mu M = 82$ ppm at 1 atm, 1000 K) flowing over Sm_2O_3 between 1000 and 1200 K. Samaria *pretreated* with CH_4 (or H_2) at reaction temperatures instantly releases N_2 when exposed to NO. Prompt CO formation also occurs on methane-conditioned samples. In contrast, stationary outflow gas compositions attain only after several reactor residence times following step ($NO + CH_4$) injections to the untreated catalyst. Nitric oxide reduction rates R_{-NO} are roughly proportional to $([CH_4] \times [NO])^{1/2}$ but do not extrapolate to zero at $[NO] \rightarrow 0$ and always increase with T. We infer that: (1) there is no direct reaction between CH_4 and NO on the catalyst surface; (2) instead, NO is reduced to N_2 by reaction with oxygen vacancies V, and with nonvolatile carbon-containing C_s species created in the heterogeneous oxidation/decomposition of CH_4, respectively; (3) the entire mass, rather than just the surface, of catalyst microparticles participate in this phenomenon. We propose a purely heterogeneous mechanism in which physisorbed NO reacts with either vacancies in equilibrium with the active oxygen O_R species responsible for CH_4 oxidation or with C_s species. The derived kinetic law: $R_{-NO} = k_A([NO]_s[CH_4])^{1/2} + k_B[CH_4]$, with $[NO]_s = [NO]/(K_8^{-1} + [NO])$, in conjunction with the reported Arrhenius parameters, closely fits rates measured under anoxic conditions. The fact that R_{-NO} is unaffected by O_2 up to $F_{O_2} \sim 0.3F_{NO}$ but drops at larger F_{O_2} inflows, even if O_2 is fully consumed in CH_4 oxidation, is consistent with the competition of NO and O_2 for vacancies. The dissimilar observations made in experiments performed in the Torr range strongly suggest that solid catalysts promote combustion at such relatively high pressures.

Introduction

Increasingly stringent regulations on nitric oxide emissions from stationary or mobile sources cannot be solely met by combustion control measures and demand effective removal technologies.[1−12] Although the thermodynamically allowed, direct decomposition of NO is the optimal strategy, current approaches rely on the selective catalytic reduction (SCR) of NO_x during the concomitant oxidation of ammonia or hydrocarbons in lean exhaust emissions. Cu and other metal-doped ZSM-5 zeolites,[3,5] a variety of metal oxides and perovskites,[8−12] and supported noble metals have all been proposed as possible catalysts for SCR. However, the implementation of SCR remains a challenge, particularly in connection with diesel engines. For example, zeolite catalysts not only undergo hydrothermal deactivation but their efficiency peaks at about 600 K. Noble metals are only active within a narrow temperature range and lead to undesirable N_2O emissions. On the other hand, many metal oxides sustain moderate activity for SCR at high temperatures in the presence of a variety of reducing agents. Recently, Zhang et al. tested several rare-earth oxide catalysts for this purpose.[8,10−12]

The conditions prevailing during the interaction of the relatively dilute exhaust gas mixtures (∼100's ppm NO) with solid catalysts obviously call for low-pressure experiments. In this paper we report a detailed investigation on the fundamental mechanism by which metal oxides catalyze SCR in low-pressure NO/hydrocarbon mixtures typical of lean combustion emissions. We chose Sm_2O_3 as a model oxide because it is relatively active for SCR,[8] and its behavior as a catalyst of hydrocarbon oxidations is well-characterized.[13−18] We find that nitric oxide is instantaneously converted into N_2 on samaria *previously* reduced under methane or hydrogen atmospheres, in a process that requires neither gas-phase (such as methyl radicals) or surface C-containing intermediates. On the other hand, the fact that NO/CH_4 mixtures approach steady-state compositions rather slowly rules out a direct reaction between the two gases on the catalyst. Both phenomena point to catalyst bulk restructuring associated with the creation of oxygen vacancy defects.[19−26] The partial reduction of samaria by CH_4 (or by any other means) generates defects that induce O_2 and NO decompositions by transferring charge into their antibonding HOMO's. We present a novel mechanism based on these ideas that quantitatively describes the kinetics of the heterogeneous decomposition of nitric oxide mediated by $Sm_2O_{3-\gamma}$.

Experimental Section

The uniformly heated (945−1200 K) flow reactor (fused silica, cylindrical, 5 cm diameter, 0.1 L), fed via a capillary inlet from a vacuum manifold, was directly connected to an on-line modulated beam mass spectrometer (Extrel). The reactor could be bypassed through a three-way valve and was mostly operated in the Knudsen flow regime. The latter is characterized by mass- and temperature-dependent residence times: $t_i = 1/k_{ei} = 9.09\ (M_i/T)^{1/2}$ (M_i is the molecular mass in daltons) of

† Dedicated to Sidney W. Benson.

10.1021/jp9812987 CCC: $15.00 © 1998 American Chemical Society
Published on Web 06/05/1998

about 1 ± 0.5 s.[13] The catalyst [ca. 1.0 g of samaria powder consisting of $\sim(3 \pm 1)$ μm diameter particles, as determined by optical microscopy, see below] was uniformly dispersed on a loosely packed silica wool support that filled the reactor. This highly porous packing increased residence times by about 20% relative to the empty reactor. Slow evacuation of the reactor (initially at atmospheric pressure, but ordinarily maintained under vacuum) through the mass spectrometer prevented blowing off the dispersed samaria powder. Reproducible kinetic results obtained over weeks confirmed the integrity of this setup. Premixed gases flowed once through the heated reactor in the following ranges: $13 < F_{CH_4}/\text{nM s}^{-1} < 6000$, $6 < F_{NO}/\text{nM s}^{-1} < 360$, leading to $[CH_4]_{ss} = F_{CH_4}t_{CH_4} < 6.9$ μM, $[NO]_{ss} < 0.56$ μM. This upper limit corresponds to 4.6×10^{-5} atm of NO, i.e., the equivalent to 46 ppm of NO at 1 atm, 1000 K. Under such conditions, reactants, products, and intermediates largely collide with surfaces, either the reactor wall or the catalyst. The fast mass spectrometric detection system (40 eV electron impact ionization) for the continuous and simultaneous monitoring of reactants and products has been described in detail previously.[13,14] It consists of a differential pumping chamber, in which a molecular beam is created from the gases exiting the reactor, a collimating orifice, and a second chamber housing a variable speed chopper, an axial electron impact ionizer, and a quadrupole mass analyzer. Signals from the electron multiplier were amplified, fed to a lock-in amplifier, filtered and acquired by a personal computer for further analysis. Mass scans could be typically programmed to sample each peak for 200 ms or longer, at a frequency of 10 Hz or smaller, depending on the time constant of the lock-in amplifier and the S/N ratio. Sm_2O_3 (Aldrich) was initially conditioned under 0.5 Torr of O_2 for several hours at 1200 K and then about 30 min at the reaction temperature between kinetic measurements. Catalyst particle sizes were determined by optical microscopy using 0.5% sodium hexametaphosphate as a dispersing agent. Methane and oxygen (high purity, AGA Argentina) were used as received. Nitric oxide was prepared by reaction of $NaNO_2$ with KI, purified by vacuum distillation at 190 K, and kept in the dark.

Results and Discussion

Reaction Products. We verified that nitric oxide decomposes slowly but measurably over samaria above 1200 K, with a half-life of ca. 25 s at 1190 K (i.e., about 16 residence times), in the absence of CH_4. Hence, the spontaneous decomposition of NO can be effectively ignored. In contrast, nitrous oxide N_2O, one of the possible species in this system, rapidly decomposes with a half-life of about 0.5 s under identical conditions. Thus, it was impossible to detect nitrous oxide as a reaction product. Mass spectra of CH_4 (62.3 nM)/NO (27.6 nM) mixtures flowing over samaria at 1100 K exhibit changes in the intensities of signals at $m/z = 18$ (H_2O), 28 (N_2 and/or CO) and 30 (NO), and the lack of other products, such as CO_2 ($m/z = 44$) or NO_2 ($m/z = 46$), that could have been readily detected (Figure 1). We verified that the packed reactor was inert in the absence of samaria. At much larger concentrations CH_4 (6.4 μM)/NO(0.55 μM), CO_2 ($m/z = 44$) appears as a product (Figure 2). In this case, the analysis of the $m/z = 28$ peak, based on previously measured *relative* response factors $(I_{N_2}/F_{N_2})/(I_{NO}/F_{NO}) = 0.72$, $(I_{CO}/F_{CO})/(I_{N_2}/F_{N_2}) = 1.24$ (the I's are mass signal intensities),[14] indicates that little CO is formed, i.e., that $\alpha \sim 1$:

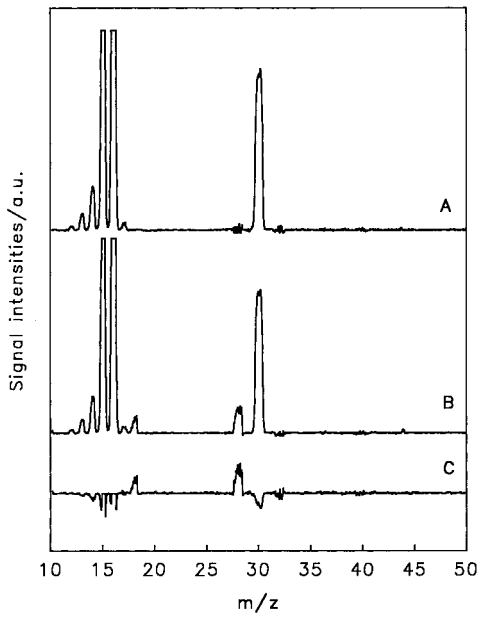

Figure 1. 40 eV mass spectra of a $CH_4/NO = 3.1$ ($F_{NO} = 1.84$ nmol s^{-1}) mixture issuing from: (A) the reactor bypass, (B) the reactor containing 1 g Sm_2O_3 at 1100 K. (C) (B − A).

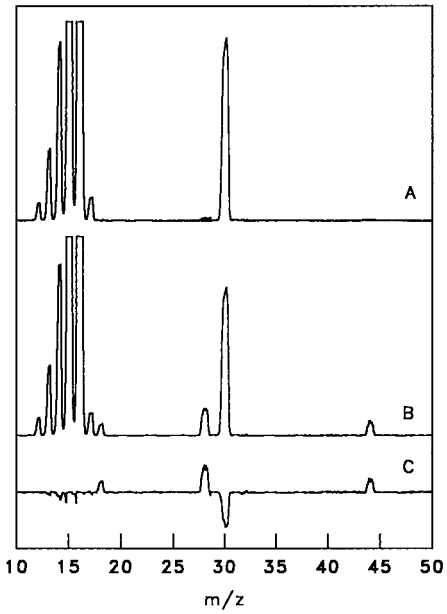

Figure 2. 40 eV mass spectra of a $CH_4/NO = 15.8$ ($F_{NO} = 37.1$ nmol s^{-1}) mixture issuing from: (A) the reactor bypass, (B) the reactor containing 1 g Sm_2O_3 at 1100 K. (C) (B − A).

$$(3 + \alpha)NO + CH_4 \Rightarrow [(3 + \alpha)/2]N_2 + (1 - \alpha)CO + \alpha CO_2 + 2H_2O \quad (1)$$

The addition of moderate amounts of O_2 ($F_{O_2} = 15.6$ nmol $s^{-1} = 0.29$ F_{NO}) to a CH_4 (4.1 μmol s^{-1})/NO (54 nmol s^{-1}) mixture does not inhibit the decomposition of nitric oxide (see Figure 3). In principle, one might ascribe this circumstance to the fact that O_2 is totally consumed (Figure 3B). To test this possibility, we increased the O_2 inflow almost 4-fold ($F_{O_2} =$ 59 nmol $s^{-1} = 1.1F_{NO}$). Now, the extent of NO decomposition drops 4.4 times and carbon dioxide becomes the dominant product (Figure 4), although O_2 is again depleted (in the deeper oxidation of a large excess of CH_4). In this case it is also possible to discern the formation of C_2-hydrocarbons (notice the fragment ions at $m/z = 26$, 27, and 29 in Figure 4) that

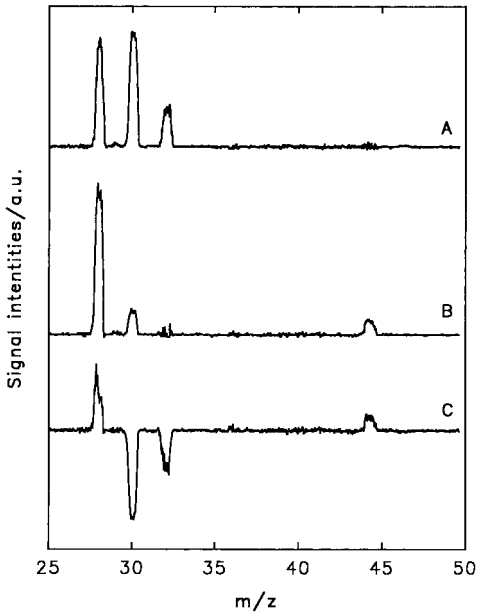

Figure 3. 40 eV mass spectra of a CH_4:NO:O_2: 76:1.0:0.29 (F_{NO} = 53.9 nmol s^{-1}) mixture issuing from: (A) the reactor bypass (some N_2 was present in the original mixture), (B) the reactor containing 1 g Sm_2O_3 at 1100 K (notice the absence of O_2). (C) B − A.

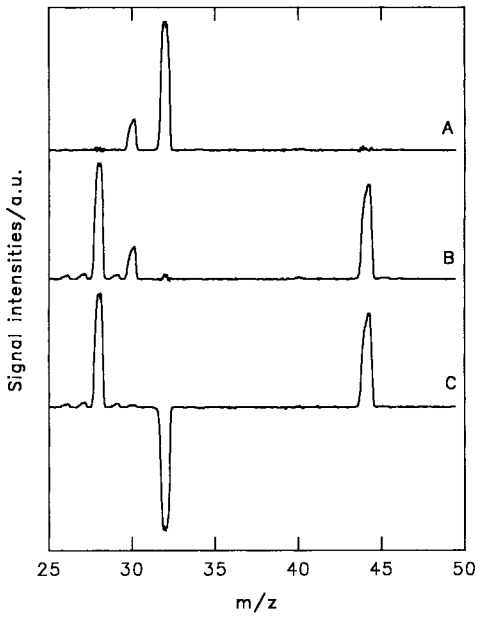

Figure 4. As in Figure 3 but for a CH_4:NO:O_2: 76:1.0:1.09 (F_{NO} = 53.9 nmol s^{-1}) mixture. Notice: (1) the full consumption of O_2, (2) the nonvanishing signals at m/z = 26, 27, and 29 in (B), (3) the negligible NO losses in (C), and (4) the relatively larger signals at m/z = 44.

result from the larger CH_3(g) concentrations associated with extensive methane oxidation. We infer that *(1) NO is largely unreactive toward (intermediate or otherwise) C-containing species formed in the heterogeneous oxidation of methane*; *(2) NO reacts instead with reduced surface sites that are competitively inactivated by O_2.* These results contrast with previous reports of experiments carried out at much larger (several Torr) concentrations and strongly implicate the occurrence of gas-phase reactions under the latter conditions.[8−12]

Transient Experiments. Step function injection of NO onto samaria that had been previously exposed for 8 min to methane at 1100 K ([CH_4] = 1830 nM), followed by an 8 min evacuation period at the same temperature, led to the results of Figure 5a.

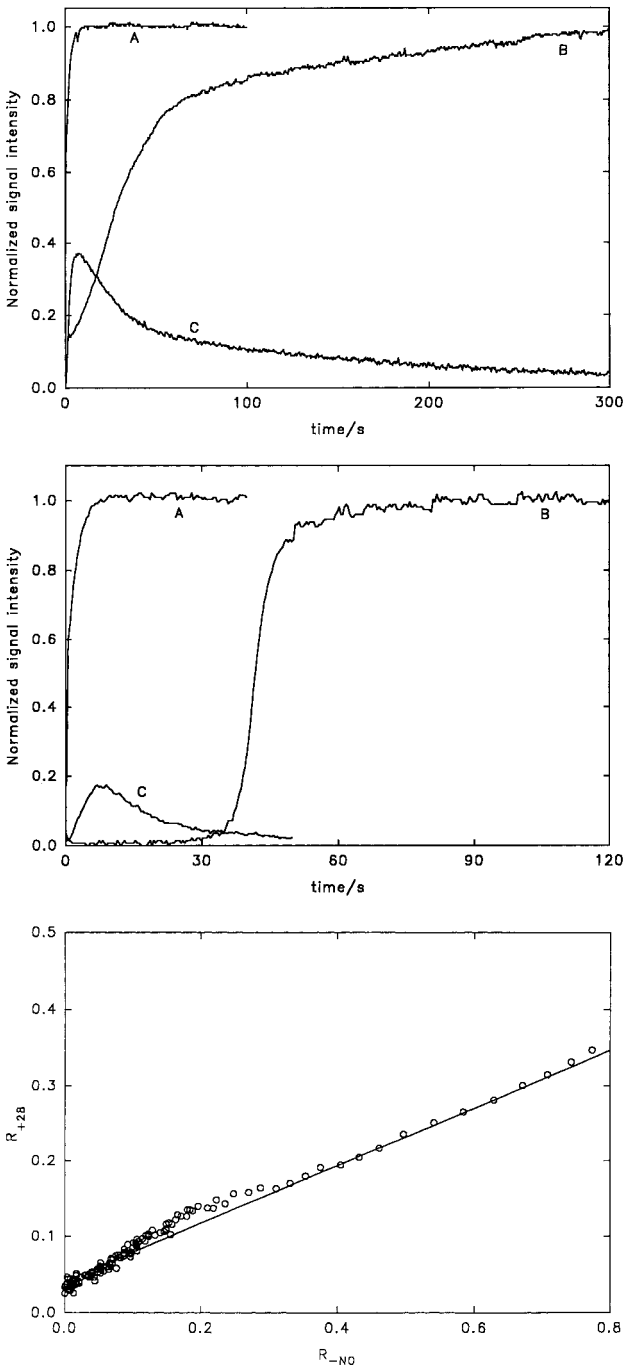

Figure 5. (a, top) (A) Intensity of the m/z = 30 signal in the gases issuing from the empty reactor upon step injection of NO (F_{NO} = 11.4 nmol s^{-1}). (B) as in (A) but from the reactor containing 1 g Sm_2O_3 that had been previously exposed 8 min to [CH_4] = 1839 nM and later evacuated for 8 min at 1 μTorr (1 Torr = 133.3 Pa) total pressure at 1100 K. (C) the m/z = 28 signal intensity of the products generated in (B). (b, middle) (A) Intensity of the m/z = 32 signal in gases issuing from the empty reactor upon step injection of O_2 (F_{O2} = 17.7 nmol s^{-1}, equivalent to 35.4 nmoles s^{-1} of NO on a per O-atom basis). (B) as in (A), but from the reactor containing 1 g Sm_2O_3 that had been previously exposed 8 min to [CH_4] = 1839 nM and later evacuated for 8 min at 1 μTorr total pressure at 1100 K. Observe that the partially reduced oxide quantitatively captures O_2 during the initial 45 s. (C) The m/z = 28 signal intensity in experiment (B). (c, bottom) Instantaneous rates R_{+28} vs R_{-NO} in Figure 5a (see Appendix 1). The linear relationship implies the simultaneous formation of N_2 and/or CO upon NO disappearance from the gas phase. The slope 0.38 corresponds to the value expected from the relative response factors of N_2 and NO and implies negligible formation of N-containing surface or gas-phase intermediates.

The prompt release of gaseous species of mass 28 indicates the fast reaction of NO with a chemically modified Sm_2O_3. A similar experiment in which NO is replaced by O_2 (Figure 5b) unambiguously confirms the creation of a substantial pool of O-vacancies in the pretreated oxide. It is also apparent that O_2 is captured more avidly than NO by the solid. The early release of small amounts of CO in the latter experiment indicates the presence of oxidizable carbonaceous surface species produced by methane decomposition, as opposed to oxidation, under anoxic conditions.[28] After being regenerated with oxygen, the oxide becomes inert toward NO.

From the $I_{30}(t)$ and $I_{28}(t)$ curves of Figure 5a it is possible to derive the instantaneous rates R_{+28}, R_{-NO} by numerical differentiation (Appendix).[15] The linearity of the plot R_{+28} vs R_{-NO} (Figure 5c) is consistent with the simultaneous formation of N_2 upon NO disappearance from the gas phase. The slope $R_{+28}/R_{-NO} = 0.38 \sim 0.72/2$ nearly coincides with the value expected from the stoichiometry $NO \Rightarrow {}^1/_2N_2$, and the relative response factors of NO and N_2 (see above). Therefore, the conversion is not only prompt but quantitative; i.e.; there is no accumulation of N-containing surface or gas-phase intermediate species. The slight departure from linearity arises from the fleeting contribution of CO to the $m/z = 28$ signal. However, the fact that NO is being reduced by the solid long after CO is released proves that there is a large pool of reactive sites that do not contain carbon. The issue of whether NO oxidizes surface carbon species directly, rather than indirectly by first filling O-atom vacancies, cannot be decided solely by the analysis of transient experiments (see below).

The above conclusions were confirmed by the fact that prior reduction of samaria with H_2, in lieu of CH_4, yields a solid that is also reactive toward NO decomposition. Exhaustive evacuation at pressures below 1 μTorr has a similar effect.[29] We routinely measure sizable stoichiometry defects ($\gamma \sim 2 \times 10^{-4}$) in $Sm_2O_{3-\gamma}$ heated above 1000 K under 1 μTorr O_2 by back-titration with O_2 at 100 mTorr.[19,29]

Kinetic Results. Steady-state decay rates R_{-j} were calculated from the expression:

$$R_{-j} = [(I_j^0 - I_j)/I_j^0]F_j \qquad (2)$$

where I_j is the intensity (in arbitrary units) of the molecular ion signal of species j in the gas exiting the reactor, I_j^0 is the corresponding signal for the gas reaching the mass spectrometer via the bypass, and the F_j is the input concentration flow rate.[17,18] We use steady-state concentrations $[X_j]$ within the reactor: $[X_j] = (t_j F_j I_j / I_j^0)$, rather than feed gas concentrations, as kinetic variables.

Rates of NO losses R_{-NO} as function of [NO] at several $[CH_4]$'s, at 1000, 1100, and 1200 K are displayed in Figures 6−8. In Figure 9a,b we show R_{-NO} vs $[CH_4]$ plots obtained at constant [NO]'s, at 1100 and 1200 K. It is apparent that R_{-NO} (1) increases with $[CH_4]$ (but less than linearly) and T, (2) increases with [NO] up to a limiting value, and (3) does not extrapolate to zero at $[NO] \rightarrow 0$. Remarkably, we found that steady-state conditions were attained long (e.g., 20 min at 1000 K) after admitting gases into the reactor, at variance with previous studies of hydrocarbon oxidations by O_2(g) on samaria in the same setup.[13−17] Considering that (1) inert gases usually reach stationary flow conditions within a couple of seconds, (2) CH_4/NO mixtures undergoing a direct reaction (*even a slow one*) on the catalyst surface would have behaved similarly, (3) neither NO or CH_4 adsorb appreciably at these high temperatures, and (4) although NO is inert, CH_4 is slowly oxidized on samaria, we ascribe the observed induction periods to a slow relaxation process in the solid phase triggered by the partial reduction of its surface. On the basis of the preceding evidence, such process must involve the propagation of surface-generated

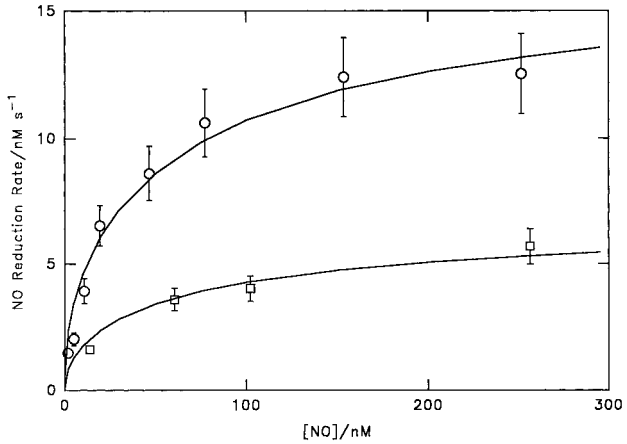

Figure 6. Rate of NO reduction over 1 g Sm_2O_3 as a function of [NO] at 1000 K. Circles: in the presence of $[CH_4] = 5400$ nM. Squares: $[CH_4] = 910$ nM. Solid lines represent nonlinear least-squares fits of eq 12 to the data and can be calculated with the parameters of eqs 13−15.

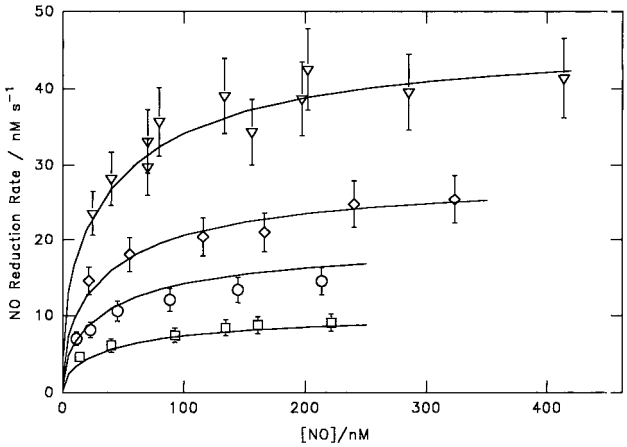

Figure 7. Rate of NO reduction over 1 g Sm_2O_3 as a function of [NO] at 1100 K. Squares: in the presence of $[CH_4] = 260$ nM. Circles: $[CH_4] = 910$ nM. Diamonds: $[CH_4] = 1830$ nM. Triangles: $[CH_4] = 4600$ nM. Solid lines represent nonlinear least-squares fits of eq 12 to the data and can be calculated with the parameters of eqs 13−15.

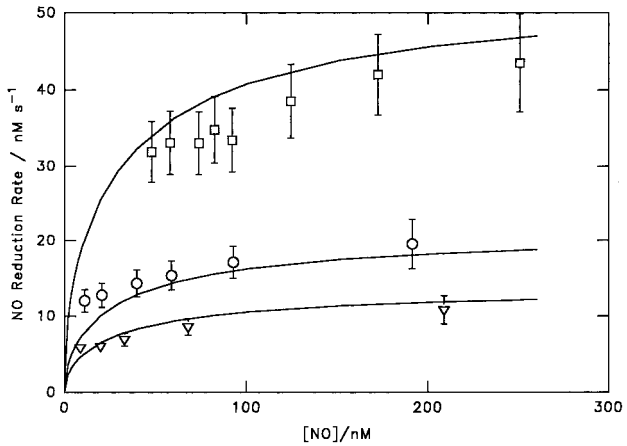

Figure 8. Rate of NO reduction over 1 g Sm_2O_3 as a function of [NO] at 1200 K. Squares: in the presence of $[CH_4] = 222$ nM. Circles: $[CH_4] = 36.5$ nM. Triangles: $[CH_4] = 15.5$ nM. Solid lines represent nonlinear least-squares fits of eq 12 to the data and can be calculated with the parameters of eqs 13−15.

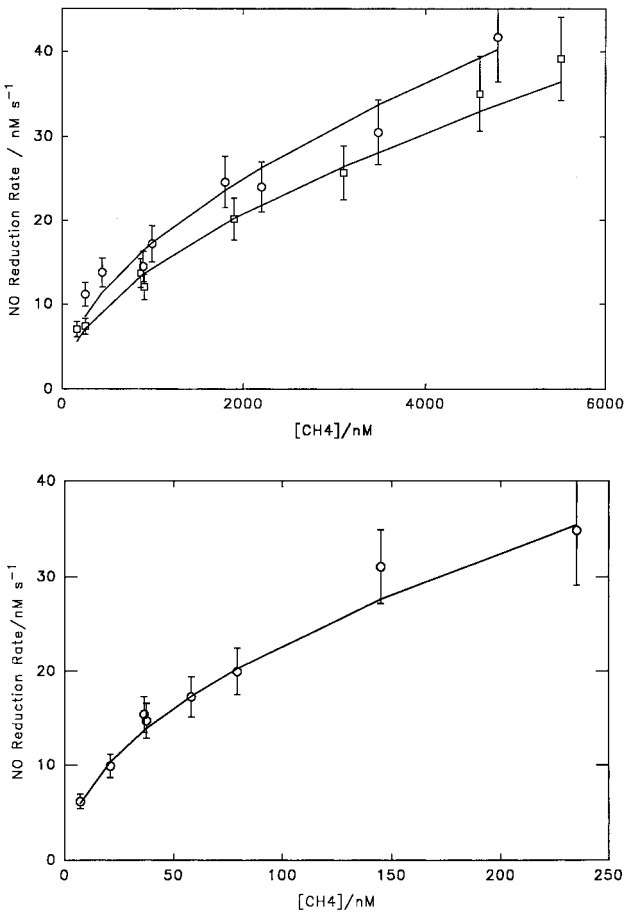

Figure 9. (a, top) Rate of NO reduction over 1 g Sm_2O_3 as a function of $[CH_4]$ at 1100 K. Squares: in the presence of [NO] = 85.2 nM. Circles: [NO] = 217 nM. Solid lines represent nonlinear least-squares fits of eq 12 to the data and can be calculated with the parameters of eqs 13−15. (b, bottom) Rate of NO reduction over 1 g Sm_2O_3 as a function of $[CH_4]$ at 1200 K in the presence of [NO] = 53.5 nM. Solid lines represent nonlinear least-squares fits of eq 12 to the data and can be calculated with the parameters of eqs 13−15.

O-atom vacancies into the core of the catalyst particles. Actually, the observed induction periods are commensurate with the characteristic times $\tau = r^2/(\pi D)$ for spreading a vacancy front via the counterdiffusion of O-atoms in monoclinic Sm_2O_3 microspheres. Thus, we estimate induction periods τ of the order of hundreds of seconds in micrometer particles, on the basis of O-atom diffusion coefficient values calculated from the expression $D_O(cm^2\ s^{-1}) = 9.2 \times 10^{-6}\ \exp(-11\,870/T)$, reported in the literature.[30]

The ratio $r = R_{-NO}/R_{-CH_4}$ varied between 2 and 4, depending on [NO], at 1200 K, where it was possible to measure both rates simultaneously. Whereas *r*-values larger than 3 are consistent with the stoichiometry of reaction 1, smaller values imply additional CH_4 losses via thermal decomposition into ($C + 2H_2$) (see below).

Kinetic and Thermochemical Constraints. Before considering possible reaction mechanisms, it is instructive to review the kinetics and thermochemistry of these reactions:

$$NO \leftrightarrow {}^1/_2O_2 + {}^1/_2N_2 \quad (3)$$

$$CH_3 + NO \leftrightarrow CH_3NO \quad (4)$$

$$CH_3 + NO \rightarrow HCN + H_2O \quad (4')$$

$$CH_3 + NO \rightarrow H_2CN + OH \quad (4'')$$

$$CH_4 \rightarrow C + 2H_2 \quad (5)$$

From $\Delta H_3 = -21.6$ kcal/mol, $\Delta S_3 = -2.9$ eu, $\Delta G_3 = -18.7$ kcal/mol, $K_3(atm) = 1.3 \times 10^4$ at 1000 K,[31] we obtain $P_{NO} = [(0.749)^{1/2}/K_3]\ P_{O_2}{}^{1/2} = 14.9$ ppm for $P_{O_2} = 0.05$ atm. The assumed P_{O_2} value corresponds to maximum O_2 levels in exhaust mixtures from the lean combustion of methane: $CH_4 + 2.73(O_2 + 4N_2) = CO_2 + 2H_2O + 0.73O_2 + 10.93N_2$. A similar calculation at a flame temperature of 1800 K leads to $K_3 = 99$, $P_{NO} = 1948$ ppm. Thus, it is sufficient to catalyze NO decomposition at temperatures below ca. 1000 K to meet emission standards.

For the equilibrium 4, with $\Delta H_4 = -39.7$ kcal/mol, $\Delta S_3 = -32.7$ eu, $\Delta G_3 = -7.0$ kcal/mol, $K_4 = 34.3\ atm^{-1}$ at 1000 K, we get $[CH_3NO]/[CH_3] = 0.017$ at 500 ppm NO. In other words, less than 2% methyl radicals could be trapped as nitrosomethane by 500 ppm NO at 1000 K, provided that total pressures are sufficiently high to stabilize the adduct. Such fraction rises up to 72% at 800 K. On the other hand, the irreversible reactions 4′ and 4″, with $\log(k_{4'} + k_{4''}$, $cm^3\ molecule^{-1}\ s^{-1}) = -24.3 + 3.52 \log T - 863/T$,[32a] i.e., $(k_{4'} + k_{4''}) = 2.5 \times 10^{-15}\ cm^3\ molecule^{-1}\ s^{-1}$ at 1000 K, lead to half-lives longer than 50 s for the decay of NO in the presence of $[CH_3] < 1 \times 10^{13}$ molecules/cm^3 ($\sim$ 1 mTorr at 1000 K). Since both channels occur by fast rearrangements of the initial CH_3-NO complex, they are effectively pressure-independent.[32b] Thus, although gas-phase methyl radicals are the direct precursors of C_2-hydrocarbons in the oxidative dimerization of methane,[9a,17] they are predictably irrelevant in the reduction of nitric oxide at low pressures. The situation may be entirely different in the fuel-rich reburning stage of emission control devices where the OH-radicals produced in the dominant channel 4″ can initiate gas-phase radical chain reactions. Since K_5 (atm) > 10 above 1000 K,[31] it is always possible to decompose methane into its elements at pressures below 0.1 atm via kinetically favorable heterogeneous pathways. We have previously reported on the occurrence of reaction 5 over samaria under anoxic conditions.[17,19]

Reaction Mechanism. On the basis of the preceding arguments we propose the following kinetic scheme:

$$O_L \leftrightarrow O_R + V \quad (6)$$

$$CH_4 + 3O_R \rightarrow CO + 2H_2O \quad (7)$$

$$NO \leftrightarrow NO_s \quad (8)$$

$$NO_s + V \rightarrow {}^1/_2N_2 + O_R \quad (9)$$

$$CH_4 \rightarrow C_s + H_2 \quad (10)$$

$$C_s + NO \rightarrow CO + {}^1/_2N_2 \quad (11)$$

where O_L and O_R are lattice and reactive oxygen species, respectively, NO_s represents physisorbed NO, and C_s denotes C-containing fragments on the surface. Pseudoelementary reaction 7 stands for the cascade oxidation of CH_4 into CO. Its overall rate is controlled by the initial step $CH_4 + O_R \rightarrow CH_3 + OH_s$.[18] Assuming that reaction 6 is in equilibrium throughout and that $[O_L]$ (the pool of lattice oxygen) is nearly constant, we get the relationship $K_6 = [O_R][V]$. The former assumption

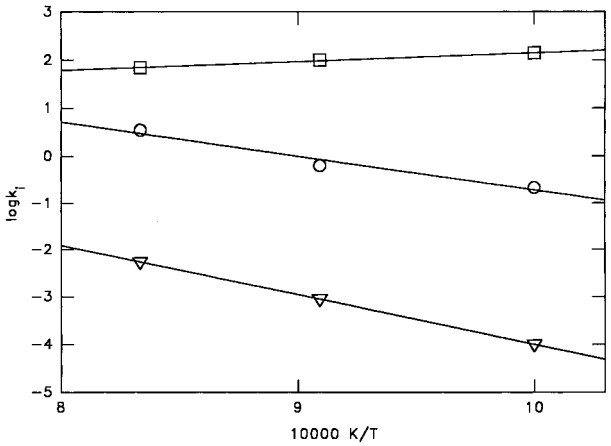

Figure 10. Arrhenius plots of k_A (circles), k_B (triangles), and K_8^{-1} (squares). The parameters are given in the text, eqs 13, 14, and 15, respectively.

is supported by the fact that $^{18}O_2$ exchanges its label without yielding $C^{18}O$ or $C^{18}O^{16}O$ in hydrocarbon oxidations on Sm_2-$16O_3$ above 1000 K,[29] i.e., that $k_{-6} \gg k_7$. Moreover, the rates of reactions 7 and 9 must obviously balance at steady state.

Therefore, from $3k_7[CH_4][O_R] = k_9[NO_s][V]$, $[O_R] = K_6/[V]$, we get $[V] = \{3K_6k_7[CH_4]/(k_9[NO_s])\}^{1/2}$ and $R_9 = k_9[NO_s][V] = (3K_6k_7k_9)^{1/2}([CH_4][NO_s])^{1/2}$. Since there cannot be net accumulation of C_s at steady state, a similar argument applies to the independent pathway comprising steps 10 and 11, i.e., $R_{11} = R_{10} = k_{10}[CH_4]$. Thus, by adding up the rates of steps 9 and 10, we obtain a three-parameter rate law for the overall rate of NO decomposition

$$R_{-NO} = k_A([NO_s][CH_4])^{1/2} + k_B[CH_4] \qquad (12)$$

where $k_A = (3K_6k_7k_9)^{1/2}$ and $k_B = k_{10}$. We assume an empirical Langmuir isotherm for NO physisorption under the reaction conditions $[NO_s] = [NO]/(K_8^{-1} + [NO])$, for lack of better information. The interesting mechanistic feature is that although CH_4/NO encounters on the surface of the catalyst are inconsequential, the overall reaction still proceeds via a process mediated by stoichiometric defects. A nonlinear least-squares fit of eq 12 to the kinetic data shown in Figures 6−9 leads to the following expressions (see Figure 10):

$$\log(k_A/\mathrm{nM}^{1/2}\ \mathrm{s}^{-1}) = (6.44 \pm 1.22) - (7169 \pm 1334)/T \quad (13)$$

$$\log(k_B/\mathrm{s}^{-1}) = (6.56 \pm 0.06) - (10580 \pm 100)/T \quad (14)$$

$$\log(K_8^{-1}/\mathrm{nM}) = (0.35 \pm 0.11) + (1800 \pm 125)/T \quad (15)$$

From these figures we estimate that NO decomposes over samaria at a rate of about 0.01 μmol s^{-1}/(g Sm_2O_3) in an equimolar NO/CH_4 mixture at 500 ppm, 1000 K in the absence of O_2. These rates will increase 20-fold at 1200 K. Assuming typical specific areas of about 1×10^5 cm^2/(g Sm_2O_3), and 5×10^{-15} cm^2/active site, we derive turnover frequencies of 3×10^{-4} and 6×10^{-3} at 1000 and 1200 K, respectively. Dispersion of samaria on high surface area inert oxides (such as alumina) may improve catalytic efficiency.[8] Since k_A involves the product $K_6k_7k_9$, the concept of a rate-determining step for the V-pathway is at least ambiguous.[33] An alternative mechanism in which C_s intermediates are oxidized by O_R rather than by NO_s leads to a rate law slightly more complex than eq 12 but does not modify the main conclusions. We consider that kinetic data alone provide insufficient evidence to decide on this issue. However, the lack of ^{18}O-labeled carbon oxides in oxidations with $^{18}O_2$ seems to confirm the proposed mechanism. Further work regarding this issue is underway.[29] On the basis of previous evidence,[13−17] the adverse effect of O_2(g) on R_{-NO} is ascribed to the establishment of the equilibrium

$$O_2\,(g) + 2V \leftrightarrow 2O_R \qquad (16)$$

that effectively competes with reaction 9 for vacancies. Summing up, present results provide decisive evidence about the central role of O-vacancies in NO reduction over metal oxides and support a general mechanism of catalysis. In this context it is interesting to point out that Lunsford et al. recently suggested that the release of oxygen at moderate temperatures may be a common feature of all active oxide catalysts for this process.[9b] Since the formation of surface O-vacancies can be promoted by O^{2-} migration in electrically conducting oxides,[24−27] our results suggest that the role of hydrocarbons in SCR over oxides is neither specific or essential. As a chemical sink for oxygen, hydrocarbon oxidation can be conceivable segregated from nitric oxide decomposition.

Conclusions

Low-pressure experiments in $NO/CH_4/O_2$ mixtures over samaria prove that NO is rapidly converted into N_2 by reaction with oxygen vacancies generated in the heterogeneous oxidation of CH_4. Although moderate ($F_{O_2}/F_{NO} \sim 0.3$) O_2 additions do not affect the extent of NO decomposition, larger amounts of O_2 inhibit the reduction of NO even if O_2 is fully consumed in CH_4 oxidation. NO is inert to gas-phase C-containing intermediates under heterogeneous conditions. Therefore, the chemistry that takes place in $NO/CH_4/O_2$ mixtures at pressures above a few Torr must be associated with gas-phase combustion processes initiated on the catalyst.

Acknowledgment. This project was financially supported by the National Research Council of Argentina (CONICET), under Grant PID1131/91.

Appendix

Let F_{NO} be the NO inflow (in nM s^{-1}) into the catalytic reactor and R_{-NO} the overall rate of reaction 1. Mass balance requires that

$$d[NO]/dt = F_{NO} - k_{30}\,[NO] - R_{-NO} \qquad (17)$$

where k_{30} is the escape rate constant of NO from the reactor. $F_{NO} = k_{30}\,[NO]_0$, where $[NO]_0$ is proportional to the I_{30}° signal, measured when the reactor is bypassed. Hence

$$R_{-NO} = k_{30}\,([NO]_0 - [NO]) - d[NO]dt \qquad (18)$$

For a reaction product of mass 28 ($I_{28}^\circ = 0$) we get

$$R_{+28} = k_{28}[28] + d[28]/dt \qquad (19)$$

Therefore, the instantaneous rates R_{-NO} and R_{+28} can be calculated from the transient signals $I_{30}(t)$, $I_{30}^\circ(t)$, $I_{28}(t)$, and their first time derivatives measured by filling the empty reactor with a step function: $F_{NO}(t) = \{F_{NO}\ (t \geq 0);\ 0\ (t < 0)\}$ (Figure 5a).[15] The linear plot of Figure 5c therefore implies negligible

accumulation of N-containing species on the surface or in the gas-phase at any time.

References and Notes

(1) Fritz, A.; Pitchon, V. *Appl. Catal. B* **1997**, *13*, 1−25.

(2) (a) Armor, J. N., Ed. *Environmental Catalysis*; ACS Symposium Series 552; American Chemical Society, Washington, D.C., 1994 and references therein. (b) Armor, J. N. *Appl. Catal. B* **1992**, *1*, 221. (c) Topsoe, N. Y. *Science* **1994**, *265*, 5176.

(3) (a) Iwamoto, M.; Yahiro, H. *Catal. Today*, **1994**, *22*, 5. (b) Iwamoto, M.; Mizuno, N.; Yahiro, H.; Taylor, K. C.; Blanco, J.; Nam, I. S.; Bartholomew, C. H.; Metcalfe, I. S.; Iglesia, E.; et al. *Stud. Surf. Sci. Catal. B* **1993**, *75*, 1285. (c) Jellinek, K. *Z. Anorg. Allg. Chem.* **1906**, *49*, 229.

(4) Cho, B. K. *J. Catal.* **1995**, *155*, 184.

(5) Iwamoto, W.; Yokoo, S.; Sakai, K.; Kagawa, S. *J. Chem. Soc., Faraday Trans. 1*, **1981**, *77*, 1629.

(6) Li, Y.; Armor, J. N. *Appl. Catal. B* **1992**, *1*, L31.

(7) Li, Y.; Hall, W. J. *J. Phys. Chem.* **1990**, *94*, 6145.

(8) Shi, C.; Walters, A. B.; Vannice, M. A., *Appl. Catal. B* **1997**, *14*, 175.

(9) (a) Xie, S.; Rosynek, M. P.; Lunsford, J. H. *Catal. Lett.* **1997**, *43*, 1. (b) Xie, S.; Mestl, G.; Rosynek, M. P.; Lunsford, J. H. *J. Am. Chem. Soc.* **1997,** *119*, 10186.

(10) Zhang, X.; Walters, A. B.; Vannice, M. A. *J. Catal.* **1994**, *146*, 568.

(11) Zhang, X.; Walters, A. B.; Vannice, M. A. *Appl. Catal. B* **1996**, *7*, 321.

(12) Zhang, X.; Walters, A. B.; Vannice, M. A. *J. Catal.* **1995**, *155*, 290.

(13) Amorebieta, V. T.; Colussi, A. J. *J. Am. Chem. Soc.* **1996**, *118*, 10236.

(14) Amorebieta, V. T.; Colussi, A. J. *J. Am. Chem. Soc.* **1995**, *117*, 3586. Although absolute response factors may be affected by total pressure, relative values are rather insensitive to such a parameter, particularly for species of similar masses.

(15) Colussi, A. J.; Amorebieta, V. T. *J. Phys. Chem.* **1995**, *99*, 13921.

(16) Amorebieta, V. T.; Colussi, A. J. *J. Phys. Chem.* **1989**, *93*, 5155.

(17) Amorebieta, V. T.; Colussi, A. J. *J. Phys. Chem.* **1988**, *92*, 4576.

(18) Colussi, A. J.; Amorebieta, V. T. *J. Catal.* **1997,** 169, 301**.**

(19) Colussi, A. J.; Amorebieta, V. T. In *Methane and Alkane Conversion Chemistry*; Bhasin, M. M., Slocum, D. W., Eds.; Plenum Press: New York, 1995; p 131.

(20) (a) Kosuge, K. *Chemistry of Nonstoichiometric Compounds;* Oxford University Press: Oxford, 1994; pp 23 ff. (b) Roberts, M. W. *Chem. Soc. Rev.* **1996**, *25*, 437.

(21) Ranga Rao, G.; Fornasiero, P.; Di Monte, R.; Kaspar, J.; Vlaic, G.; Balducci, G.; Meriani, S.; Gubitosa, G.; Cremona, A.; and Graziani, M. *J. Catal.* **1996**, *162*, 1.

(22) Winter, E. R. S. *J. Catal.* **1971**, *22*, 158.

(23) Hightower, J. W.; van Leirburg, D. A. In *The Catalytic Chemistry of Nitric Oxides*; Klimisch, R. L., Larson, J. G., Eds.; Plenum: New York, 1975.

(24) Marina, O. A.; Yentekakis, I. V.; Vayenas, C. G.; Palermo, A.; Lambert, R. M., *J. Catal.* **1997**, *166*, 218.

(25) Chien, C. C.; Shi, J. Z.; Huang, T. J. *Ind. Eng. Chem. Res.* **1997**, *36*, 1544.

(26) Yasuda, H.; Nitadori, T.; Mizuno, N.; Misono, M. *Bull. Chem. Soc. Jpn.* **1993**, *66*, 3492.

(27) Baker, D. R.; Verbrugge, M. W. *J. Electrochem. Soc.*, **1996,** *143*, 2396.

(28) (a) Shangguan, W. F.; Teraoka, Y.; Kagawa, S., *Appl. Catal. B* **1997**, *12*, 237. (b) Connerton, J.; Joyner, R. W.; Stockenhuber, M. *Chem. Commun.* **1997**, 185.

(29) Amorebieta, V. T.; Colussi, A. J. In preparation.

(30) Stone, G. D.; Weber, G. R.; Eyring, L. *Natl. Bur. Stand. (U.S.) Spec. Publ.* **1968**, *296*, 179.

(31) NIST Standard Reference Database 25, version 2.02; National Bureau of Standards and Technology: Gaithersburg, MD, 1994.

(32) (a) Miller, J. A.; Melius, C. F.; Glarborg, P. *Int. J. Chem. Kinet.* **1998**, *30*, 223. (b) Hennig, G.; Wagner, Gg. H., *Ber. Bunsen-Ges. Phys. Chem.*, **1994**, *98*, 749.

(33) Cowan, A. D.; Dümpelmann, R.; Cant, N. W. *J. Catal.* **1995**, *151*, 356.